

Track-Before-Detect Procedures in Clutter Environments

Danilo Orlando, Luca Venturino, Marco Lops, and Giuseppe Ricci

Abstract—In this paper we propose and assess TBD strategies for radar systems adopting STAP. At the design stage we consider a radar system equipped with a linear array of N_a sensors that illuminates the surveillance area by transmitting M coherent pulse trains, each consisting of N_p pulses, before deciding whether or not a target is present over L adjacent range cells. As a preliminary step we introduce the target and noise models. Then, resorting to GLRT and ad hoc procedures, we derive adaptive CFAR detectors for both stationary and scan-to-scan varying clutter scenarios (a point better clarified in the body of the paper). The proposed detectors guarantee the CFAR property with respect to the unknown spectral properties of the clutter. The preliminary performance assessment, conducted resorting to Monte Carlo simulation, shows that proposed procedures might be a viable means to implement early detection and track initiation of weak moving targets.

Index Terms—Space-Time Adaptive Processing (STAP), Constant False Alarm Rate (CFAR), Generalized Likelihood Ratio Test (GLRT), Track-Before-Detect (TBD), Viterbi Algorithm.

I. INTRODUCTION

IN traditional tracking systems a set of point measurements is obtained by thresholding the received baseband signal at the output of a matched filter. Then, the tracking algorithm links such measurements across time and estimates the parameters of interest. The threshold value must be low enough to guarantee a sufficiently high probability of target detection. However, a low threshold gives rise to a high rate of false alarms. To avoid false tracks, a data association problem must be solved [1], and a reliable means of validating the track estimates is also required.

For low signal-to-noise-ratio (SNR) targets, solving the data association problem may become a formidable task. An alternative approach, referred to as track-before-detect (TBD), consists of feeding the processor with unthresholded data. TBD-based procedures jointly process more consecutive scans (or frames) and, relying on a target kinematics or, simply, exploiting the physically admissible target transitions, jointly declare the presence of a target and, eventually, its track. A TBD algorithm can improve track accuracy and follow low SNR targets. Moreover, a TBD scheme ensuring the constant false alarm rate (CFAR) property with respect to the unknown statistics of the disturbance controls the overall false track acceptance probability (CFAR property at the track level). The

D. Orlando, L. Venturino and M. Lops are with the DAEIMI, Università degli Studi di Cassino, Via G. Di Biasio 43, I-03043 Cassino (Fr), Italy. E-Mail: danilo.orlando@unisalento.it, [l.venturino, lops]@unicas.it.

G. Ricci is with the Dipartimento di Ingegneria dell'Innovazione, Università del Salento, Via Monteroni, 73100 Lecce (Le), Italy. E-Mail: giuseppe.ricci@unisalento.it.

main problem with TBD techniques is that the measurements depend on the target kinematics in a highly nonlinear way [2], [3], [4]. We refer the readers to [5] for a comparison of several different TBD strategies to detect low amplitude targets.

Most of TBD algorithms have been proposed to detect and track small moving objects in optical images corrupted by high cluttered noise. Their use in connection with radar systems has received less attention: for a description of the existing results see [6], [7]. Observe that in the radar scenario the tracking problem involves (at least in principle) optimization in a four-dimensional (4-D) parameter space, whose dimensions are range, Doppler shift, azimuth, and elevation angles, rather than in a 2-D one as in the optical framework, making the complexity requirement much more stringent. Also, the clutter environment may rapidly change. Thus, it is crucial in radar applications to develop low-complexity adaptive algorithms.

In this paper we extend the derivation of [7] to the context of space-time adaptive processing (STAP). In particular, we consider a radar system equipped with a linear array of N_a sensors which illuminates the surveillance area by transmitting M coherent pulse trains, each consisting of N_p pulses, before deciding whether or not a target is present over L consecutive range cells. As a preliminary step we introduce the target and noise models. Then, resorting to both the generalized likelihood ratio test (GLRT) [8] and *ad hoc* procedures, we derive adaptive CFAR detectors assuming either a *scan-to-scan* varying scenario (where the unknown clutter covariance matrix can possibly change from scan to scan) or a *stationary* scenario (where the unknown clutter covariance matrix remains constant during the entire observation time). Simulations results are also provided to assess and compare the performances of the proposed strategies.

II. PROBLEM FORMULATION

Let us consider a radar system equipped with a uniform linear array of N_a sensors with inter-element spacing d . During the m -th scan, the following train of N_p pulses is transmitted:

$$\Re e \left\{ A e^{j\varphi} \sum_{n=1}^{N_p} p(t - (n-1)T - (m-1)\Delta) e^{j2\pi f_c t} \right\}, \quad (1)$$

with $t \in [(m-1)\Delta, (m-1)\Delta + N_p T)$ and $m = 1, \dots, M$. In (1), $\Re e \{z\}$ indicates the real part of the complex number z , $A > 0$ is an amplitude factor related to the transmitted power, $\varphi \in [0, 2\pi)$ is the initial phase of the carrier signal, $p(t)$ is a unit-energy rectangular pulse waveform of duration T_p and one-sided bandwidth $W_p \approx 1/T_p$, T is the pulse

repetition time, $\text{PRF} = 1/T$ is the pulse repetition frequency, $\Delta \geq N_p T$ is the scan repetition time; finally, $f_c = c/\lambda$ is the carrier frequency, where c is the velocity of propagation in the medium (assume that $c = 3 \cdot 10^8$ m/sec) and λ is the carrier wavelength.

We assume that a prospective target is located in the antenna far zone and has a radial velocity v_m during the m -th scan ($v_m > 0$ if the target is approaching the radar). Neglecting compression or stretching of the time scale of the transmitted pulses, the complex envelope of the received signal at the i -th sensor and over the m -th scan is given by [9]

$$r_m^i(t) = \alpha_m e^{j2\pi(i-1)\nu_{sm}} e^{j2\pi f_m t} \times \sum_{n=1}^{N_p} p(t - (n-1)T - (m-1)\Delta - \tau_m) + w_m^i(t), \quad (2)$$

for $i = 1, \dots, N_a$ and $m = 1, \dots, M$. In (2), $\alpha_m \in \mathbb{C}$ is a factor which accounts for target and channel effects; τ_m is the round-trip delay time of the received signal; f_m is the Doppler frequency shift of the signal backscattered by the target, given by $f_m = f_c 2v_m/c$; $\nu_{sm} = (d/\lambda) \cos \psi_m$ is the target spatial frequency, with $\cos \psi_m$ the direction cosine of the impinging wave with respect to the array axis; finally, $w_m^i(t)$ is the complex envelope of the overall disturbance component.

As customary, a discrete form for the signal received at the i -th sensor is obtained by sampling at pulse repetition time the output of a filter matched to $p(t)$ and fed by $r_m^i(t)$ in (2). The interested reader is referred to [9], [10] for a detailed description of the discrete-time model and of the involved approximations. Summarizing, the radar collects $N = N_a \times N_p$ samples from the l -th range cell, $l = 1, \dots, L$, at the m -th scan, $m = 1, \dots, M$; we will denote by z_{lm} the N -dimensional vector of noisy returns obtained by stacking up the (N_p -dimensional) vectors collected at the N_a sensors.

Finally, the problem of deciding whether or not a target occupies the l -th range gate amounts to solving the following binary hypothesis testing problem¹

$$\begin{cases} H_0 : z_{lm} = \mathbf{n}_{lm}, & \forall l, m, \\ H_1 : \begin{cases} z_{lm} = \alpha_m \mathbf{v}(\nu_m, \nu_{sm}) + \mathbf{n}_{lm}, & l = l_m, \forall m, \\ z_{lm} = \mathbf{n}_{lm}, & l \neq l_m, \forall m, \end{cases} \end{cases} \quad (3)$$

where α_m is a proper modification of the previous constant; the \mathbf{n}_{lm} 's are assumed to be independent and identically distributed (iid) complex normal random vectors with zero-mean and unknown covariance matrix $\mathbf{R}_m \in \mathbb{C}^{N \times N}$, i.e., $\mathbf{n}_{lm} \sim \mathcal{CN}_N(\mathbf{0}, \mathbf{R}_m)$; $\nu_m = f_m/\text{PRF}$ is the normalized Doppler frequency of the target; finally, $\mathbf{v}(\cdot, \cdot)$ is the space-time steering vector. For estimation purposes we will assume that² $L - 1 \geq N$.

III. DETECTOR DESIGNS

In this section we propose GLRT-based adaptive procedures to solve the composite binary hypothesis testing problem (3).

¹Observe that the expression for the discrete-time signal under H_1 is correct only if there is no spillover of target energy to adjacent matched filter samples.

²Observe that such assumption might not be met in realistic scenarios.

At the design stage, l_m , ν_m , α_m , and \mathbf{R}_m are modeled as unknown deterministic parameters that must be estimated from the observables. In particular, we assume that $\alpha_1 \neq \dots \neq \alpha_M$: this accounts for the fact that the radar cross section of the moving target and/or the channel response may change from scan to scan. Moreover, in order to limit the computational burden (but conceptually without any loss of generality) we assume that $\psi_m = \psi$, $m = 1, \dots, M$, and that ψ is known at the receiver. As a consequence, we can neglect the dependence of the space-time steering vector on ν_{sm} .

As to the external environment, instead, we consider both a *scan-to-scan* varying scenario where the unknown clutter covariance matrix changes from scan to scan (i.e., $\mathbf{R}_1 \neq \dots \neq \mathbf{R}_M$) and a *stationary* scenario where the unknown clutter covariance matrix remains constant from scan to scan (i.e., $\mathbf{R}_1 = \dots = \mathbf{R}_M$). As to the target parameters, we denote by $\mathcal{D} = \{(l_1, \nu_1), \dots, (l_M, \nu_M)\} \in \mathcal{S}$ the sequence of points occupied by a prospective target in the Range-Doppler domain, where \mathcal{S} is the set of all physically admissible target trajectories [7]. Finally, for future reference, we indicate by $\boldsymbol{\alpha} = [\alpha_1 \dots \alpha_M] \in \mathbb{C}^{1 \times M}$ the row vector of target responses and by $\mathbf{Z} = [z_{11} \dots z_{L1} \dots z_{1M} \dots z_{LM}] \in \mathbb{C}^{N \times ML}$ the overall data matrix.

A. One-step GLRT-based detector

Assume here that $\mathbf{R}_1 \neq \dots \neq \mathbf{R}_M$. The GLRT for problem (3) is given by

$$\frac{\max_{\mathcal{D} \in \mathcal{S}} \max_{\boldsymbol{\alpha}} \max_{\mathbf{R}_1, \dots, \mathbf{R}_M} f_1(\mathbf{Z}; \mathcal{D}, \boldsymbol{\alpha}, \mathbf{R}_1, \dots, \mathbf{R}_M)}{\max_{\mathbf{R}_1, \dots, \mathbf{R}_M} f_0(\mathbf{Z}; \mathbf{R}_1, \dots, \mathbf{R}_M)} \underset{H_0}{\overset{H_1}{>}} \gamma, \quad (4)$$

where γ is a detection threshold to be set in order to ensure the desired probability of false alarm (P_{fa}), while

$$f_0(\mathbf{Z}; \mathbf{R}_1, \dots, \mathbf{R}_M) = \prod_{m=1}^M \left[\frac{1}{\pi^N \det(\mathbf{R}_m)} \right]^L \times \exp \left\{ -\text{tr} \left[\mathbf{R}_m^{-1} \left(z_{l_m m} z_{l_m m}^\dagger + \mathbf{S}_{l_m m} \right) \right] \right\} \quad (5)$$

and

$$f_1(\mathbf{Z}; \mathcal{D}, \boldsymbol{\alpha}, \mathbf{R}_1, \dots, \mathbf{R}_M) = \prod_{m=1}^M \left[\frac{1}{\pi^N \det(\mathbf{R}_m)} \right]^L \times \exp \left\{ -\text{tr} \left[\mathbf{R}_m^{-1} \left(\mathbf{X}_{l_m m}(\nu_m) + \mathbf{S}_{l_m m} \right) \right] \right\} \quad (6)$$

are the probability density functions (pdfs) of the received data under H_0 and H_1 , respectively. In (5) and (6), $\det(\cdot)$ and $\text{tr}(\cdot)$ are the determinant and the trace of a square matrix, respectively, $(\cdot)^\dagger$ denotes the conjugate transpose, and

$$\mathbf{X}_{l_m m}(\nu_m) = (z_{l_m m} - \alpha_m \mathbf{v}(\nu_m)) (z_{l_m m} - \alpha_m \mathbf{v}(\nu_m))^\dagger, \quad \mathbf{S}_{l_m m} = \sum_{\substack{l=1 \\ l \neq l_m}}^L z_{lm} z_{lm}^\dagger. \quad (7)$$

Notice that the matrix $\mathbf{S}_{l_m m}$ in (7) is $L - 1$ times the sample covariance matrix of the clutter based on the available data over the m -th scan, but for the l_m -th cell.

It is not difficult to show that equation (4) can be re-written in the following form [8]

$$\max_{\mathcal{D} \in \mathcal{S}} \sum_{m=1}^M \log \frac{1 + \mathbf{z}_{l_m m}^\dagger \mathbf{S}_{l_m m}^{-1} \mathbf{z}_{l_m m}}{1 + \mathbf{z}_{l_m m}^\dagger \mathbf{S}_{l_m m}^{-1/2} \mathbf{P}_{l_m m}^\perp(\nu_m) \mathbf{S}_{l_m m}^{-1/2} \mathbf{z}_{l_m m}} \underset{H_0}{\overset{H_1}{>}} \gamma, \quad (8)$$

where

$$\mathbf{P}_{l_m m}^\perp(\nu_m) = \mathbf{I}_N - \frac{\mathbf{S}_{l_m m}^{-1/2} \mathbf{v}(\nu_m) \mathbf{v}(\nu_m)^\dagger \mathbf{S}_{l_m m}^{-1/2}}{\mathbf{v}(\nu_m)^\dagger \mathbf{S}_{l_m m}^{-1} \mathbf{v}(\nu_m)}$$

is a projection matrix onto the orthogonal complement of the space spanned by $\mathbf{S}_{l_m m}^{-1/2} \mathbf{v}(\nu_m)$ and \mathbf{I}_N is the N -dimensional identity matrix.

As a final remark, we point out that the derivation of the GLRT for stationary scenarios appears not feasible since maximization with respect to vector α cannot be carried out in a closed-form at authors' knowledge.

B. Ad hoc detectors

In this subsection we derive ad hoc detectors for both considered scenarios modifying the GLRT-based design procedure.

Assume first that $\mathbf{R}_1 \neq \dots \neq \mathbf{R}_M$. If the covariance matrices of the noise are known, the GLRT is tantamount to the following decision rule

$$\frac{\max_{\mathcal{D} \in \mathcal{S}} \max_{\alpha} f_1(\mathbf{Z}; \mathcal{D}, \alpha, \mathbf{R}_1, \dots, \mathbf{R}_M)}{f_0(\mathbf{Z}; \mathbf{R}_1, \dots, \mathbf{R}_M)} \underset{H_0}{\overset{H_1}{>}} \gamma, \quad (9)$$

where $f_0(\cdot; \cdot)$ and $f_1(\cdot; \cdot)$ are given by equations (5) and (6), respectively. After maximizing with respect to α , the GLRT (9) becomes

$$\max_{\mathcal{D} \in \mathcal{S}} \sum_{m=1}^M \frac{|\mathbf{v}(\nu_m)^\dagger \mathbf{R}_m^{-1} \mathbf{z}_{l_m m}|^2}{\mathbf{v}(\nu_m)^\dagger \mathbf{R}_m^{-1} \mathbf{v}(\nu_m)} \underset{H_0}{\overset{H_1}{>}} \gamma. \quad (10)$$

Finally, to come up with a fully-adaptive detector, we replace \mathbf{R}_m with $1/(L-1)\mathbf{S}_{l_m m}$ in the above equation to yield

$$\max_{\mathcal{D} \in \mathcal{S}} \sum_{m=1}^M \frac{|\mathbf{v}(\nu_m)^\dagger \mathbf{S}_{l_m m}^{-1} \mathbf{z}_{l_m m}|^2}{\mathbf{v}(\nu_m)^\dagger \mathbf{S}_{l_m m}^{-1} \mathbf{v}(\nu_m)} \underset{H_0}{\overset{H_1}{>}} \gamma. \quad (11)$$

On the other hand, if $\mathbf{R}_1 = \dots = \mathbf{R}_M = \mathbf{R}$, test (10) simplifies to

$$\max_{\mathcal{D} \in \mathcal{S}} \sum_{m=1}^M \frac{|\mathbf{v}(\nu_m)^\dagger \mathbf{R}^{-1} \mathbf{z}_{l_m m}|^2}{\mathbf{v}(\nu_m)^\dagger \mathbf{R}^{-1} \mathbf{v}(\nu_m)} \underset{H_0}{\overset{H_1}{>}} \gamma. \quad (12)$$

In this latter case, a fully adaptive detector could be in principle obtained from (12) by replacing \mathbf{R} with

$$\hat{\mathbf{R}}(\mathcal{D}) = \frac{1}{(L-1)M} \sum_{m=1}^M \sum_{\substack{l=1 \\ l \neq l_m}}^L \mathbf{z}_{l m} \mathbf{z}_{l m}^\dagger.$$

However, such strategy would require evaluating (and above all inverting) a different sample covariance matrix for each

feasible target trajectory. A more practical solution, instead, is to replace \mathbf{R} with the sample covariance matrix based upon the overall data set, namely

$$\hat{\mathbf{R}} = \frac{1}{ML} \sum_{m=1}^M \sum_{l=1}^L \mathbf{z}_{l m} \mathbf{z}_{l m}^\dagger. \quad (13)$$

The main drawback of (13) is that for very high SNR values the presence of data contaminated by useful signal components has a detrimental effect on the detection performance of the corresponding decision scheme³ [12]. However, such a behavior is not a real concern since we are primarily interested in low SNR scenarios. An alternative and computationally-efficient solution that overcomes such a data contamination problem is presented in the next section.

IV. IMPLEMENTATION ISSUES

This section is aimed at discussing some implementation issues concerning the above proposed TBD algorithms. In fact, (8), (10), and (12) are time consuming since they require maximization with respect to the sequence \mathcal{D} of pairs (l_m, ν_m) . As to the adaptive implementation of (12) we also have to overcome the effects of data contamination due to (13).

We first investigate an efficient way of maximizing over \mathcal{D} . To this end, observe that

- the Doppler parameter ν_m takes on values in a continuous set and the corresponding maximizer cannot be determined in a closed-form;
- maximization over \mathcal{D} cannot be conducted separately with respect to each (l_m, ν_m) pair: indeed, physical constraints on the target trajectory imply that (l_{m+1}, ν_{m+1}) depends upon $\{(l_1, \nu_1), \dots, (l_m, \nu_m)\}$ for $m = 1, \dots, M-1$.

However, partitioning the unambiguous Doppler region as

$$\Omega_D = \left\{ 0, \frac{1}{rN_p}, \frac{2}{rN_p}, \dots, \frac{rN_p - 1}{rN_p} \right\}, \quad r \in \mathbb{N},$$

leads to an optimization problem that can be solved constructing an expanded trellis diagram, whose states are the elements of $\Omega = \Omega_R \times \Omega_D$, with $\Omega_R = \{1, \dots, L\}$. Hence, we can effectively resort to a Viterbi-like procedure to find the best path metric in this expanded trellis as suggested in [7]. The Viterbi algorithm requires determining (at most) LrN_p paths in the expanded trellis diagram of depth M , with a maximum complexity⁴ $\mathcal{O}(LrN_p M)$ (linear in the number of scans).

In addition, if we restrict our attention to cases where an unambiguous Doppler estimation is not feasible (see also [7]), we can eliminate the Doppler parameter before scan-to-scan integration by maximizing each summand with respect to $\nu_m \in \Omega_D$. With this simplification in mind, it is possible

³Such ad hoc detector can be thought of as derived resorting to the two-step GLRT-based design procedure, see also [11].

⁴We resort to the usual Landau notation.

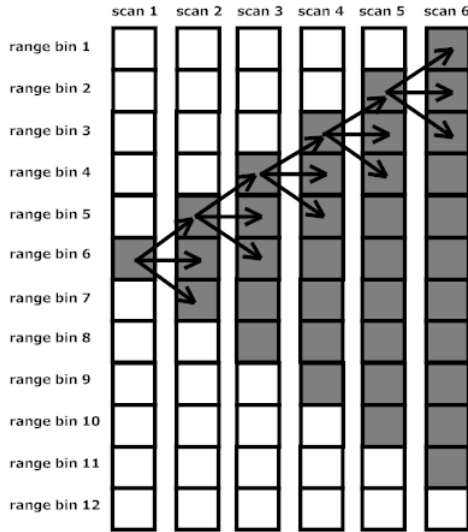


Fig. 1. Admissible target transitions among consecutive scans for $p = 1$, $L = 12$ and $l_1 = 6$.

to recast the space-time adaptive receivers (8) and (11) as

$$\max_{\substack{(l_1, \dots, l_M) \in \Omega_R^M \\ l_m \in \mathcal{P}(l_{m-1})}} \sum_{m=1}^M \max_{\nu_m \in \Omega_D} \left\{ \log \left[1 + \mathbf{z}_{l_m m}^\dagger \mathbf{S}_{l_m m}^{-1} \mathbf{z}_{l_m m} \right] \right. \\ \left. - \log \left[1 + \mathbf{z}_{l_m m}^\dagger \mathbf{S}_{l_m m}^{-1/2} \mathbf{P}_{l_m m}^\perp(\nu_m) \mathbf{S}_{l_m m}^{-1/2} \mathbf{z}_{l_m m} \right] \right\} \underset{H_0}{\overset{H_1}{>}} \gamma \quad (14)$$

and

$$\max_{\substack{(l_1, \dots, l_M) \in \Omega_R^M \\ l_m \in \mathcal{P}(l_{m-1})}} \sum_{m=1}^M \max_{\nu_m \in \Omega_D} \frac{|\mathbf{v}(\nu_m)^\dagger \mathbf{S}_{l_m m}^{-1} \mathbf{z}_{l_m m}|^2}{\mathbf{v}(\nu_m)^\dagger \mathbf{S}_{l_m m}^{-1} \mathbf{v}(\nu_m)} \underset{H_0}{\overset{H_1}{>}} \gamma, \quad (15)$$

respectively, where $\mathcal{P}(l_{m-1})$ denotes the set of elements of Ω_R that can be reached from l_{m-1} under an upperbound V_{\max} on the target radial velocity [7]. It is also worth pointing out that in this case the complexity of the search algorithm is $\mathcal{O}(LM)$. Following the same line of reasoning, detector (12) becomes

$$\max_{\substack{(l_1, \dots, l_M) \in \Omega_R^M \\ l_m \in \mathcal{P}(l_{m-1})}} \sum_{m=1}^M \max_{\nu_m \in \Omega_D} \frac{|\mathbf{v}(\nu_m)^\dagger \mathbf{R}^{-1} \mathbf{z}_{l_m m}|^2}{\mathbf{v}(\nu_m)^\dagger \mathbf{R}^{-1} \mathbf{v}(\nu_m)} \underset{H_0}{\overset{H_1}{>}} \gamma. \quad (16)$$

As already stated for detector (12) coupled with (13), also detector (16) coupled with (13) experiences detection losses for very high SNR values. To overcome this drawback, we now present an adaptive implementation of (16) in stationary clutter environments whose performance does not degrade for increasingly large SNR's. To this end, observe from Figure 1 that all physically admissible trajectories of a target occupying the l_1 -th range bin during the first scan must belong to a "cone", namely are such that

$$l_m \in \Omega_m(l_1) = \{l_1 - (m-1)p, \dots, l_1 + (m-1)p\},$$

for $m = 1, \dots, M$, where we have indicated with p the maximum allowable number of range-cell transitions between

consecutive scans (tied to V_{\max}). It follows that \mathbf{R} can be efficiently estimated by resorting to the data of the complement of such a cone, i.e.,

$$\widehat{\mathbf{R}}(l_1) = \frac{1}{M[1 + p(M-1)]} \sum_{m=1}^M \sum_{\substack{l=1 \\ l \notin \Omega_m(l_1)}}^L \mathbf{z}_{lm} \mathbf{z}_{lm}^\dagger. \quad (17)$$

Observe that the computational complexity of (16) coupled with (17) is in between that of (16) coupled with (13) and the one of detector (15).

As a final remark, it can be easily shown that detectors (14) and (15) always ensures the CFAR property with respect to $\mathbf{R}_1, \dots, \mathbf{R}_M$, while (16) coupled with (13) or (17) possesses the CFAR property with respect to the covariance matrix of the noise only when $\mathbf{R}_1 = \dots = \mathbf{R}_M = \mathbf{R}$.

V. PERFORMANCE ANALYSIS

Since closed-form expressions for the probability of detection (P_d) and the P_{fa} are not available, we resort to standard Monte Carlo counting techniques. More precisely, we estimate P_{fa} and P_d by resorting to $100/P_{fa}$ and 10^4 independent trials, respectively.

Due to the large number of involved parameters a thorough performance analysis would be a formidable task. Hereafter, we just focus on a simplified case study aimed at showing the pros and cons of the proposed algorithms. We consider a radar system with $N_a = 4$, $d = \lambda/2$, $M = 6$, $L = 32$, and rectangular pulse trains with $T_p = 0.2 \mu\text{sec}$, $N_p = 4$, PRF = 800 Hz, $r = 4$, and $\Delta = 12T$. The nominal steering vector at the m -th scan is given by

$$\mathbf{v}(\nu_m) = \frac{1}{\sqrt{N}} \begin{bmatrix} 1 \\ e^{j2\pi\nu_m} \\ \vdots \\ e^{j2\pi(N_p-1)\nu_m} \end{bmatrix} \otimes \begin{bmatrix} 1 \\ e^{j2\pi\nu_{sm}} \\ \vdots \\ e^{j2\pi(N_a-1)\nu_{sm}} \end{bmatrix},$$

where \otimes denotes the Kronecker product. As to the threshold, it is set in order to guarantee $P_{fa} = 10^{-4}$.

At the design stage, we assume $V_{\max} = 680 \text{ m/s}$ ($\approx \text{Mach-2}$) which results in at most $p = 1$ range-cell transitions between consecutive scans. The ambiguous Doppler information is eliminated before scan-to-scan integration as discussed in Section IV. As to the target, we assume a constant velocity model with $v_m \approx 680 \text{ m/s}$ and $\psi = \pi/2$.

A. Stationary environment: $\mathbf{R}_m = \mathbf{R}$, $m = 1, \dots, M$.

We assume that $\mathbf{R} = \sigma_n^2 \mathbf{I}_N + \sigma_c^2 \mathbf{C}$ and that the correlation coefficient between the clutter sample received from the k -th array element, corresponding to the n -th transmitted pulse, and the clutter sample received from the i -th array element, corresponding to the m -th transmitted pulse, namely the $((k-1)N_p + n, (i-1)N_p + m)$ entry of the matrix \mathbf{C} , is given by [13]

$$\mathbf{C}((k-1)N_p + n, (i-1)N_p + m) = \rho_s((i-k)d)\rho_t((m-n)T)$$

where $\rho_s(\Delta x) = e^{-(\Delta x)^2/(2\sigma_x^2)}$ and $\rho_t(\Delta t) = e^{-(\Delta t)^2/(2\sigma_t^2)}$ are spatial and temporal correlations with σ_x and σ_t such that the spatial and temporal one-lag correlation coefficients are equal to 0.95 and 0.97, respectively. In addition, we assume that $\sigma_n^2 = 1$ and that the clutter-to-noise ratio is equal to 20 dB (i.e., $\sigma_c^2 = 100$).

In Fig. 2 we plot P_d versus SNR for the adaptive receivers (14), (15), (16) coupled with (13), and (16) coupled with (17). The figure assumes non-fluctuating targets with the following definition for the SNR

$$\text{SNR} = |\alpha_m|^2 \mathbf{v}(\bar{\nu}_m)^\dagger \mathbf{R}^{-1} \mathbf{v}(\bar{\nu}_m),$$

where $\bar{\nu}_m$ is the actual normalized Doppler frequency of the target at the m -th scan. For comparison purposes, we also report the performance of the GLRT-based detector for known spectral properties of the clutter which is given by (16) and the performances of (14) and (15) with $M = 1$. Inspection of the figure highlights that detector (16), coupled with estimator (13) or (17), ensures a limited loss (about 0.8 dB at $P_d = 0.9$) with respect to the detector that assumes knowledge of \mathbf{R} . The figure also highlights that TBD strategies can guarantee significant gains with respect to more conventional approaches that return a decision concerning the presence of the target at each scan. However, recall that if the stationary assumption is not met, detector (16), coupled with (13) or (17), is no longer CFAR.

In Figure 3, we analyze the proposed detectors in terms of the probability of detection and tracking (P_{DT}), defined as the probability to detect the target and to estimate its track within a pre-assigned accuracy (measured in terms of maximum cell distance δ between the estimated and the true range cell at each scan). Again, performances of detector (16), coupled with (13) or (17), are very close to those of the detector for known spectral properties of the clutter.

B. Scan-to-scan varying environment: $\mathbf{R}_1 \neq \dots \neq \mathbf{R}_M$.

In this subsection we show the performance of the proposed algorithms when the noise covariance matrix changes from scan to scan. We assume for the \mathbf{R}_m 's the same structure used in the previous subsection for \mathbf{R} ; in addition, in order to come up with different covariance matrices from scan to scan, the sequence of temporal and spatial one-lag correlation coefficients are drawn from highly correlated random processes that take on values close (and less than) 0.95 and 0.97, respectively; in addition, Monte Carlo trials assume independent realizations of such processes. Figures 4 and 5 confirm that the performance hierarchy of the previous case study remains substantially unvaried. The result is not surprising since detectors designed for scan-to-scan varying scenarios use a smaller number of "training data" than detectors designed for stationary scenarios. However, notice that the latter are no longer CFAR (although the plotted curves refer to the nominal P_{fa}).

VI. CONCLUSIONS

In this paper we have proposed and assessed TBD strategies in the context of space-time adaptive processing. We

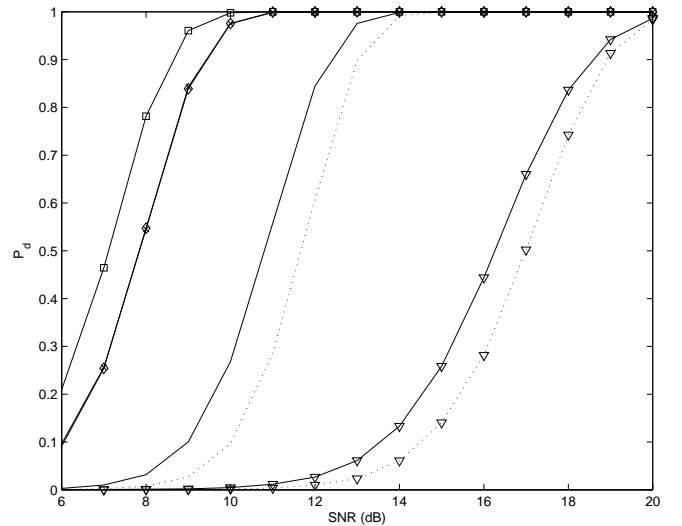


Fig. 2. P_d versus SNR assuming $\mathbf{R}_m = \mathbf{R}$, $m = 1, \dots, M$. GLRT-based detector for known spectral properties of the clutter, given by (16): square marker and solid line; GLRT-based detector for scan-to-scan varying scenario, given by (14): no marker and solid line; adaptive detector for scan-to-scan varying scenario, given by (15): no marker and dotted line; adaptive detector for stationary scenario, given by (16) coupled with (13): cross marker and solid line; adaptive detector for stationary scenario, given by (16) coupled with (17): diamond marker and solid line; GLRT-based detector, given by (14), for $M = 1$: triangle marker and solid line; ad hoc detector, given by (15), for $M = 1$: triangle marker and dotted line.

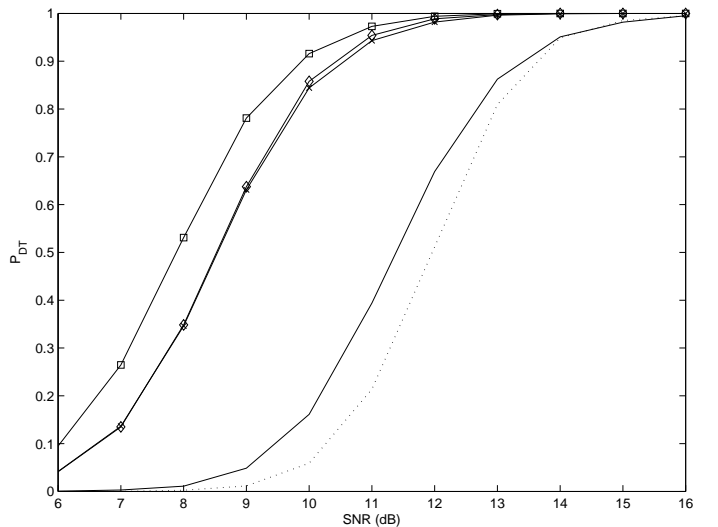


Fig. 3. P_{DT} versus SNR assuming $\mathbf{R}_m = \mathbf{R}$, $m = 1, \dots, M$, and $\delta = 0$. GLRT-based detector for known spectral properties of the clutter, given by (16): square marker and solid line; GLRT-based detector for scan-to-scan varying scenario, given by (14): no marker and solid line; adaptive detector for scan-to-scan varying scenario, given by (15): no marker and dotted line; adaptive detector for stationary scenario, given by (16) coupled with (13): cross marker and solid line; adaptive detector for stationary scenario, given by (16) coupled with (17): diamond marker and solid line.

resorted to both the GLRT and ad hoc procedures to derive CFAR detectors for either the case that the unknown clutter covariance matrix is the same over all the scans (stationary scenario) or possibly different from scan to scan (scan-to-scan

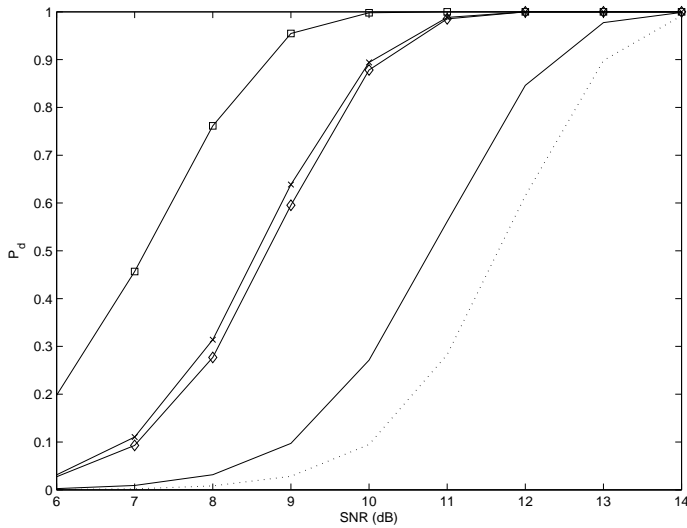


Fig. 4. P_d versus SNR assuming $R_1 \neq \dots \neq R_M$. GLRT-based detector for known spectral properties of the clutter: square marker and solid line; GLRT-based detector for scan-to-scan varying scenario, given by (14): no marker and solid line; adaptive detector for scan-to-scan varying scenario, given by (15): no marker and dotted line; adaptive detector for stationary scenario, given by (16) coupled with (13): cross marker and solid line; adaptive detector for stationary scenario, given by (16) coupled with (17): diamond marker and solid line.

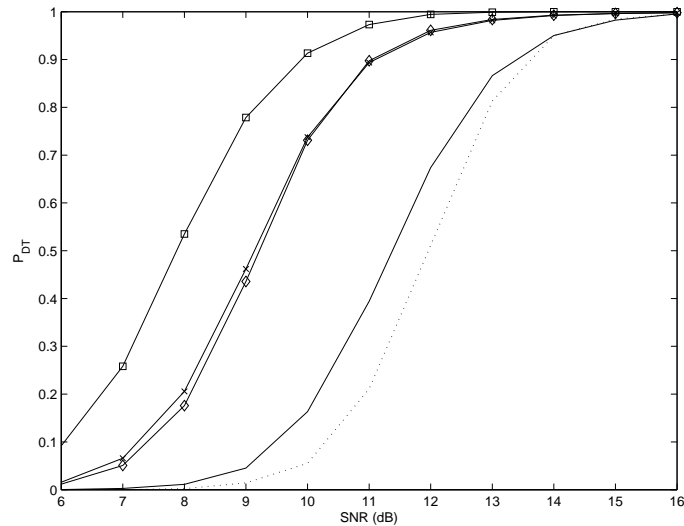


Fig. 5. P_{DT} versus SNR assuming $R_1 \neq \dots \neq R_M$ and $\delta = 0$. GLRT-based detector for known spectral properties of the clutter: square marker and solid line; GLRT-based detector for scan-to-scan varying scenario, given by (14): no marker and solid line; adaptive detector for scan-to-scan varying scenario, given by (15): no marker and dotted line; adaptive detector for stationary scenario, given by (16) coupled with (13): cross marker and solid line; adaptive detector for stationary scenario, given by (16) coupled with (17): diamond marker and solid line.

varying scenario). The preliminary performance assessment, conducted resorting to Monte Carlo simulation, has shown that knowledge of the operating environment (whether stationary or scan-to-scan varying) is of fundamental importance. In fact, detectors derived assuming the stationary scenario outperform those derived for the scan-to-scan varying one when both are

fed by stationary data; in addition, the former are less time demanding than the latter from the computational point of view. However, if the stationary assumption is not met, the former are no longer CFAR processors. Thus, we are currently investigating the possibility to model the noise in terms of autoregressive processes in order to relax the stationary assumption. Remarkably, modeling non-stationary disturbance in terms of autoregressive processes would also reduce the computational load.

REFERENCES

- [1] Y. Bar-Shalom, T. E. Fortmann, *Tracking and data association*, Academic Press, 1988.
- [2] B. Ristic, S. Arulampalam, and N. J. Gordon, *Beyond the Kalman filter: particle filters for tracking applications*, Artech House 2004.
- [3] S. M. Tonissen and Y. Bar-Shalom, "Maximum likelihood track-before-detect with fluctuating target amplitude," *IEEE Trans. on Aerospace and Electronic Systems*, Vol. 34, No. 3, pp. 796-809, July 1998.
- [4] L. A. Johnston and V. Krishnamurthy, "Performance analysis of a dynamic programming track before detect algorithm," *IEEE Trans. on Aerospace and Electronic Systems*, vol. 38, no. 1, pp. 228-242, Jan. 2002.
- [5] S. J. Davey, M. G. Rutten, and B. Cheung, "A comparison of detection performance for several track-before-detect algorithms," *EURASIP Journal on Advances in Signal Processing*, Vol. 2008, Article ID 428036, 10 pages.
- [6] W. R. Wallace, "The use of track-before-detect in pulse-doppler radar," in *Proc. IEEE 2002 International Radar Conference*, Edinburgh, UK, Oct. 2002, pp. 315-319.
- [7] S. Buzzi, M. Lops, and L. Venturino, "Track-before-detect procedures for early detection of moving target from airborne radars," *IEEE Trans. on Aerospace and Electronic Systems*, Vol. 41, No. 3, pp. 937-954, July 2005.
- [8] E. J. Kelly, "An adaptive detection algorithm," *IEEE Trans. on Aerospace and Electronic Systems*, Vol. 22, No. 2, pp. 115-127, March 1986.
- [9] J. Ward, "Space-time adaptive processing for airborne radar," MIT, Lexington, Tech. Rep. No. 1015, December 13, 1994.
- [10] F. Bandiera, D. Orlando, and G. Ricci "Advanced Radar Detection Schemes Under Mismatched Signal Models," *Synthesis Lectures on Signal Processing No. 8*, Morgan & Claypool Publishers, March 2009.
- [11] F. C. Robey, D. L. Fuhrman, E. J. Kelly, and R. Nitzberg, "A CFAR adaptive matched filter detector," *IEEE Trans. on Aerospace and Electronic Systems*, Vol. 29, No. 1, pp. 208-216, January 1992.
- [12] K. Gerlach, "The effect of signal contamination on two adaptive detectors," *IEEE Trans. on Aerospace and Electronic Systems*, Vol. 31, No. 1, pp. 297-309, January 1995.
- [13] S. Barbarossa and A. Farina, "Space-time-frequency processing of synthetic aperture radar signals," *IEEE Trans. on Aerospace and Electronic Systems*, Vol. 30, No. 2, pp. 341-358, April 1994.